

August 13, 2010

## Correction to the incident photon energy for g8b data

M. Dugger

*Arizona State University, Tempe, AZ 85287-1504*

C. Hanretty

*Florida State University, Tallahassee, FL 32306-4350*

The algorithm for a simple iterative routine to determine the correction to incident photon energies using g1c and g8b data is presented. Comparison of the results for g1c data is compared to the correction found by the CMU group. The results for g8b data is verified by the FSU group.

### I. INTRODUCTION

The energy correction presented in this document assumes that the angles measured by the CLAS detector are correct. This assumption of correctness in angle measurement allows the determination of momentum and energy correction factors from a set of four equations with four unknowns within the constraints of momentum and energy conservation using the reaction  $\gamma p \rightarrow p \pi^- \pi^+ Y$ . The document describes the reaction of interest, the iterative algorithm, and verification of results by the kinematic fitting routine of FSU.

### II. THE EVENTS OF INTEREST

The reaction of interest for this study is  $\gamma p \rightarrow p \pi^- \pi^+ Y$ . To determine if a given event is of the desired reaction: 1) each event is processed through GPID for determination of particle ID for each particle within the event; 2) the event must have one proton, one  $\pi^+$ , and one  $\pi^-$  with no other identified particles, and 3) the event, once determined to be of the type  $\gamma p \rightarrow p \pi^- \pi^+ Y$  must have a missing mass squared ( $\text{mass}^2(Y)$ ) between -0.01 and 0.00385 (see Fig. 1).

The events for g1c come from the 3.115 GeV full-tagger data set. The events for g8b come from the entire amorphous data set. The momentum of the proton was restricted such that only events with a proton momentum greater than

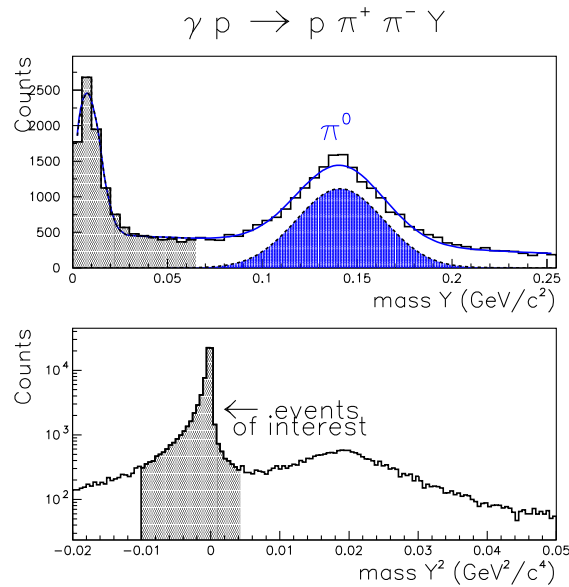


FIG. 1: Top panel is counts versus mass  $Y$  from the reaction  $\gamma p \rightarrow p \pi^- \pi^+ Y$ , and the bottom panel is counts versus mass  $Y$  squared. The events of interest in this study are shaded in black. (The  $\pi^0$  is shaded in blue.)

0.9 GeV/c were accepted for analysis. The energy corrections coming from the ELOSS package are turned off and there are no momentum corrections applied for either glc or g8b data.

### III. FUNDAMENTAL ASSUMPTION

Assume: For any measured momentum vector  $\vec{P}_{MEASURED}$  within an event,  $\vec{P}_{TRUE} = \alpha \vec{P}_{MEASURED}$ , where  $\alpha$  is a constant (i.e. The measured angle is assumed to be the same as the true angle).

### IV. FOUR EQUATIONS AND FOUR UNKNOWNNS

We start with the four-vector equation:

$$P_\gamma^\mu + P_i^\mu = P_f^\mu + P_{\pi^+}^\mu + P_{\pi^-}^\mu, \quad (1)$$

where the subscript denotes the particle type (Note: subscript  $i \rightarrow$  initial proton, and  $f \rightarrow$  final proton, with the rest being self explanatory), and the superscript denotes coordinate. We can expand this as:

$$\alpha_f P_f^x + \alpha_{\pi^+} P_{\pi^+}^x + \alpha_{\pi^-} P_{\pi^-}^x = 0 \quad (2)$$

$$\alpha_f P_f^y + \alpha_{\pi^+} P_{\pi^+}^y + \alpha_{\pi^-} P_{\pi^-}^y = 0 \quad (3)$$

$$\alpha_f P_f^z + \alpha_{\pi^+} P_{\pi^+}^z + \alpha_{\pi^-} P_{\pi^-}^z = \alpha_\gamma E_\gamma \quad (4)$$

$$\sqrt{\alpha_f^2 \vec{P}_f^2 + m_p^2} + \sqrt{\alpha_{\pi^+}^2 \vec{P}_{\pi^+}^2 + m_{\pi^+}^2} + \sqrt{\alpha_{\pi^-}^2 \vec{P}_{\pi^-}^2 + m_{\pi^-}^2} - m_p = \alpha_\gamma E_\gamma, \quad (5)$$

where the  $\alpha$  terms bring the measured values to be true values,  $m$  is the mass of the particle (type defined by the subscript),  $E_\gamma \equiv P_\gamma^t$ , and  $\vec{P}^2 = (P^x)^2 + (P^y)^2 + (P^z)^2$ .

In what follows we pick out the variable  $\alpha_f$  to be approximated by a Taylor series. The calculations and iterations were performed for two cases: 1)  $\alpha_f$  approximated, and 2)  $\alpha_{\pi^+}$  approximated. The end results did not depend on which case was chosen.

#### A. Stage 1

Define:  $\kappa_+ \equiv \frac{\alpha_{\pi^+}}{\alpha_f}$ ,  $\kappa_- \equiv \frac{\alpha_{\pi^-}}{\alpha_f}$ , and  $\kappa_\gamma \equiv \frac{\alpha_\gamma}{\alpha_f}$ . This implies a solution of Eqn. 2 and 3 in terms of  $\kappa_+$  and  $\kappa_-$ :

$$\begin{pmatrix} \kappa_+ \\ \kappa_- \end{pmatrix} = \frac{-1}{P_{\pi^+}^x P_{\pi^-}^y - P_{\pi^+}^y P_{\pi^-}^x} \begin{bmatrix} P_{\pi^-}^y & -P_{\pi^-}^x \\ -P_{\pi^+}^y & P_{\pi^+}^x \end{bmatrix} \begin{pmatrix} P_f^x \\ P_f^y \end{pmatrix}. \quad (6)$$

This is stage 1: find  $\kappa_+$  and  $\kappa_-$ .

#### B. Stage 2

From Eqn. 4 we can determine  $\kappa_\gamma$ :

$$\kappa_\gamma = \frac{P_f^z + \kappa_+ P_{\pi^+}^z + \kappa_- P_{\pi^-}^z}{E_\gamma} \quad (7)$$

This is stage 2: find  $\kappa_\gamma$ .

#### C. Stage 3

The final stage is to determine  $\alpha_f$ . First we rewrite 5 and define  $f(\alpha_f)$ :

$$f(\alpha_f) \equiv \sqrt{\vec{P}_f^2 + \left(\frac{m_p}{\alpha_f}\right)^2} + \sqrt{\kappa_{\pi^+}^2 \vec{P}_{\pi^+}^2 + \left(\frac{m_{\pi^+}}{\alpha_f}\right)^2} + \sqrt{\kappa_{\pi^-}^2 \vec{P}_{\pi^-}^2 + \left(\frac{m_{\pi^-}}{\alpha_f}\right)^2} - \frac{m_p}{\alpha_f} = \kappa_\gamma E_\gamma.$$

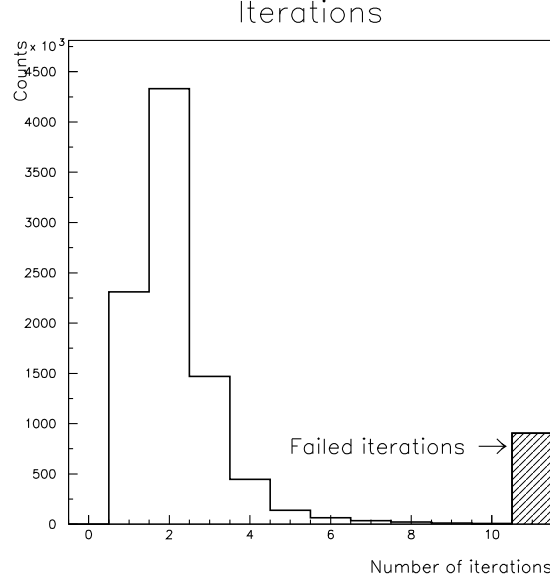


FIG. 2: iterations

Expand  $f(\alpha_f)$  in Taylor series about  $\alpha_f = 1$ :

$$f(\alpha_f) = f(\alpha_f = 1) + \frac{f'(\alpha_f = 1)}{1!}(\alpha_f - 1) + \frac{f''(\alpha_f = 1)}{2!}(\alpha_f - 1)^2 + \dots$$

Assume that  $(\alpha_f - 1)^2 \approx 0$ , so that

$$f(\alpha_f) \approx \left[ \sqrt{\vec{P}_f^2 + m_p^2} + \sqrt{\kappa_{\pi+}^2 \vec{P}_{\pi+}^2 + m_{\pi+}^2} + \sqrt{\kappa_{\pi-}^2 \vec{P}_{\pi-}^2 + m_{\pi-}^2} - m_p \right] - \left[ \frac{m_p^2}{\sqrt{\vec{P}_f^2 + m_p^2}} + \frac{m_{\pi+}^2}{\sqrt{\kappa_{\pi+}^2 \vec{P}_{\pi+}^2 + m_{\pi+}^2}} + \frac{m_{\pi-}^2}{\sqrt{\kappa_{\pi-}^2 \vec{P}_{\pi-}^2 + m_{\pi-}^2}} \right] (\alpha_f - 1). \quad (8)$$

Now, since  $f(\alpha_f) = \kappa_\gamma E_\gamma$ , we can determine  $\alpha_f$  from Eqn. 8 :

$$\alpha_f \approx \left[ \frac{-\kappa_\gamma E_\gamma + E_f + E'_{\pi+} + E'_{\pi-} - m_p}{\frac{m_p^2}{E_f} + \frac{m_{\pi+}^2}{E'_{\pi+}} + \frac{m_{\pi-}^2}{E'_{\pi-}} - m_p} \right] + 1, \quad (9)$$

where  $E_f = \sqrt{\vec{P}_f^2 + m_p^2}$ ,  $E'_{\pi+} \equiv \sqrt{\kappa_{\pi+}^2 \vec{P}_{\pi+}^2 + m_{\pi+}^2}$ , and  $E'_{\pi-} \equiv \sqrt{\kappa_{\pi-}^2 \vec{P}_{\pi-}^2 + m_{\pi-}^2}$ .

The remaining  $\alpha$ -factors can be easily found:  $\alpha_{\pi+} = \alpha_f \kappa_+$ , and  $\alpha_{\pi-} = \alpha_f \kappa_-$ .

## V. ITERATE

The routine passes through stages 1 through 3. Once stage 3 has completed, corrections are applied to the momentum and energies. After the corrections are applied, the routine goes back to stage 1 and starts all over again. This continues until each  $\alpha_n$  within an iterative step  $n$  ( $\alpha_{f,n}$ ,  $\alpha_{\pi+,n}$ ,  $\alpha_{\pi-,n}$ , and  $\alpha_{\gamma,n}$ ) has a value between 0.9999 and 1.0001, or that the routine has reached a maximum of 10 iterations. Figure 2 shows the number of iterations before successful completion, where events that show 11 iterations represent failed events. The failed events represent less than 10% of the total number of events.

Allowing for a second subscript to denote the iteration, we can write the relation between an observable (here we chose  $\vec{P}_f$  as an example) and the corrected value at each iteration, assuming that the event has a total number of  $n$

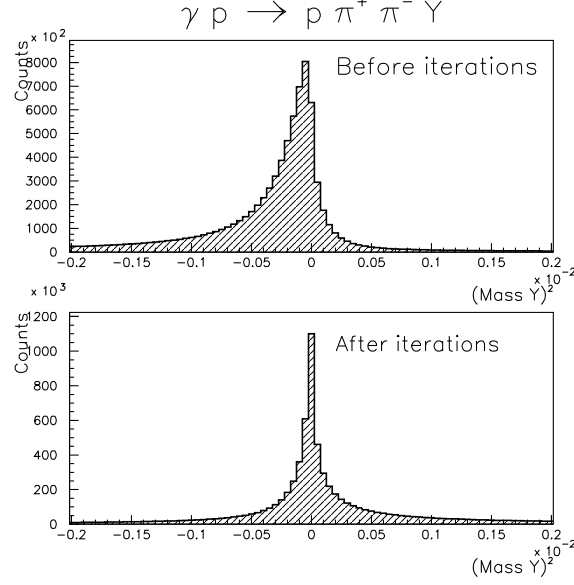


FIG. 3: Top panel: Mass  $Y$  squared before iteration. Bottom panel: Mass  $Y$  squared after iteration. Events for each panel are from the events of interest within the g8b data that also successfully complete the iterative routine.

iterations:

$$\begin{aligned}
 \vec{P}_{f,1} &= \alpha_{f,1} \vec{P}_{f,0} \\
 \vec{P}_{f,2} &= \alpha_{f,2} \vec{P}_{f,1} = \alpha_{f,2} \alpha_{f,1} \vec{P}_{f,0} \\
 &\vdots \\
 \vec{P}_{f,n} &= \alpha_{f,n} \vec{P}_{f,n-1} = \alpha_{f,n} \alpha_{f,n-1} \vec{P}_{f,n-2} = \cdots = \alpha_{f,n} \alpha_{f,n-1} \cdots \alpha_{f,1} \vec{P}_{f,0}
 \end{aligned} \tag{10}$$

If the event has terminated successfully, then  $P_{f,TRUE}$  is equated as  $P_{f,n}$  and  $\alpha_f = \alpha_{f,n} \alpha_{f,n-1} \cdots \alpha_{f,1}$ , or more simply  $\alpha_f = P_{f,n}/P_{f,0}$ .

## VI. RESULTS

The distribution of  $\text{mass}^2(Y)$  before and after the iterative routine using g8b data can be found in Fig. 3. (The results for g1c data look very similar to Fig. 3.) The iterated events are clearly better distributed about  $\text{mass}(Y) = 0$  than the non-iterated events.

The final values of  $\alpha_\gamma$  from events that successfully terminated within the iterative routine are placed in a histogram with z-coordinate representing counts, y-coordinate representing  $\alpha_\gamma$ , and x-coordinate representing  $E_\gamma$  (see left panel of Fig. 4). This 2-d histogram is then sliced into energy bins with width = 0.025 GeV and each slice fit with a Gaussian plus first degree polynomial (see right panel of Fig. 4 for an example fit). For each slice, the center of the Gaussian is taken as the value of  $\alpha_\gamma$ . From these values of  $\alpha_\gamma$  ( $\alpha_\gamma = E_{\gamma,TRUE}/E_{\gamma,MEASURED}$ ) we can determine the value of  $E_{\gamma,TRUE}$  for each energy slice.

### A. Comparison of g1c data to CMU

For g1c data, an energy correction attributable to a “sag” in the focal plane of the bremsstrahlung photon tagger was found. The energy correction due to tagger-sag was parametrized by the CMU group in a CLAS-Note [1].

The CMU tagger-sag energy correction function is given by

$$\Gamma_{TRUE} = a_0 + a_1 \Gamma + a_2 \Gamma^2, \tag{11}$$

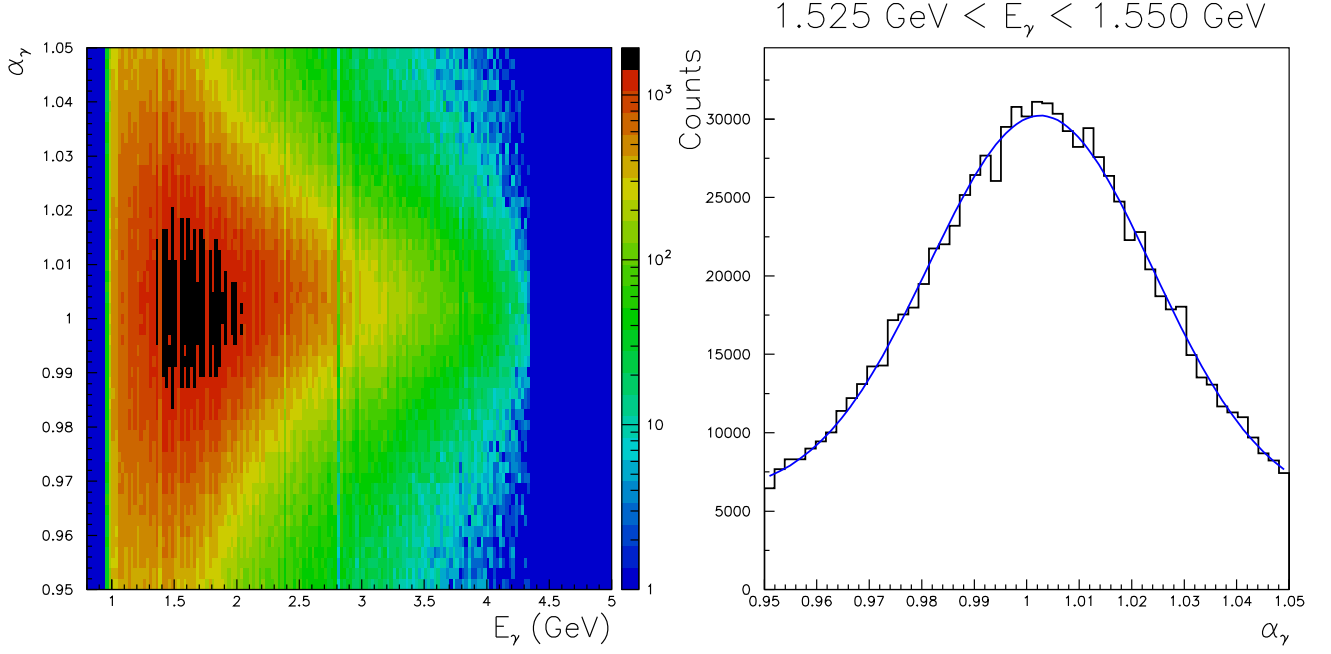


FIG. 4: Left panel: Histogram of  $\alpha_\gamma$  vs.  $E_\gamma$  Right panel: Slice 30 from histogram on left ( $\alpha_\gamma$  for  $1.525 < E_\gamma < 1.550$ ). Blue line is a Gaussian + first degree polynomial.

where  $\Gamma = E_\gamma/E_e + \nu$ ,  $\Gamma_{TRUE} \equiv E_{\gamma,TRUE}/E_e$ ,  $E_e$  is the pre-bremsstrahlung electron energy,  $\nu$  is a free parameter to be fit to data, and

$$\begin{aligned}
 a_0 &= \begin{cases} -0.00599597, & \Gamma < 0.401 \\ -0.0181293, & 0.401 \leq \Gamma \leq 0.674 \\ -0.0511162, & \Gamma > 0.674 \end{cases} \\
 a_1 &= \begin{cases} 1.0390912, & \Gamma < 0.401 \\ 1.0675599, & 0.401 \leq \Gamma \leq 0.674 \\ 1.138208, & \Gamma > 0.674 \end{cases} \\
 a_2 &= \begin{cases} -0.0573218, & \Gamma < 0.401 \\ -0.0541268, & 0.401 \leq \Gamma \leq 0.674 \\ -0.0867757, & \Gamma > 0.674 \end{cases}
 \end{aligned}$$

are fixed constants.

A comparison of the data to the energy correction obtained by the algorithm detailed in this report can be found in the left panel of Fig. 5. The right panel in Fig. 5 shows the results from the CMU CLAS-Note [1]. The results are clearly similar.

### B. Energy correction for g8b data

For the algorithm reported here, we decided to parameterize the correction for g8b data in terms of a tagger-sag function that was modified (compared to Eqn. 11) to be

$$\Gamma_{TRUE} = a_0 + a_1\Gamma + a_2\Gamma^2 + \frac{E_\gamma}{E_e}b, \quad (12)$$

where the new parameter  $b$  is needed to obtain a reasonable fit to g8b data, and all other variables and parameters are defined as in the previous subsection. The fit parameters obtained from Eqn. 12 and the g8b data are

$$\begin{aligned}
 \nu &= 0.00134, \text{ and} \\
 b &= -0.0035,
 \end{aligned}$$

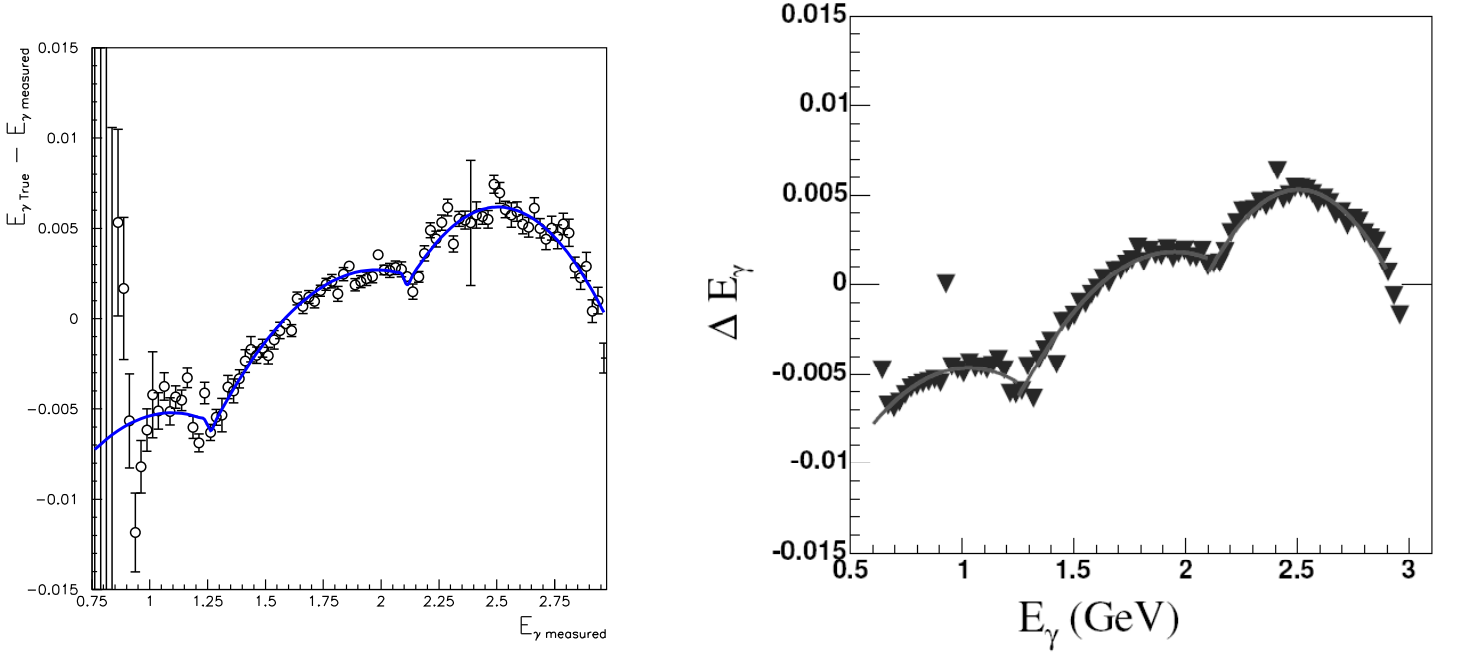


FIG. 5: Left panel:  $(E_{\text{True}} - E_{\text{Measured}})$  vs.  $E_{\text{Measured}}$  determined by the algorithm detailed here for g1c data. Right panel:  $(E_{\text{True}} - E_{\text{Measured}})$  vs.  $E_{\text{Measured}}$  determined by the CMU kinematic fitter for g1c data. The lines are from the CMU tagger-sag function [1] given in Eqn. 11.

and the fit result can be seen as the blue line in the left panel of Fig. 6.

NOTE: Recently it was determined that the value of  $E_e$  used to fit the g8b data was 4.55 instead of the more accurate value of 4.559. We determined that end results would not benefit enough by changing the value of  $E_e$  to warrant refitting the g8b results.

### C. Verification of g8b results using the FSU kinematic fitter

The pull parameters from the FSU kinematic fitter before, and after, the energy correction have been applied are in table I. The pull distribution are much better after the applied energy correction. In particular, the photon energy pull becomes reasonable after the energy correction. Previous to the energy correction, the photon energy pull variance was very bad ( $\sigma_{\text{before}} = 1.219$  and  $\sigma_{\text{after}} = 1.040$ ).

The  $E_{\gamma}$  pull distributions (before and after) are shown in the lower left panel of Fig. 7. The top right panel of Fig. 7 shows the energy dependence of the energy-corrected and uncorrected  $E_{\gamma}$  pull distributions.

Once the FSU kinematic fitter (with energy corrections applied) has converged, the resulting value for  $E_{\gamma}$  is labeled as  $E_{\text{True}}$  and the difference  $[E_{\text{True}} - E_{\text{Measured}}]$  is determined. The resulting distribution of  $[E_{\text{True}} - E_{\text{Measured}}]$  versus  $E_{\text{Measured}}$  is shown in the left hand panel of Fig. 8. As can be seen in the plot, the distribution is well centered and has widths on the order of 1 MeV. The Right hand panel gives the Distribution of a fixed value of  $E_{\text{Measured}} = 1.3$  GeV. The physical E-id from the tagging system has an energy width of about  $\pm 2$  MeV and this width is compatible with the distribution shown. An energy-difference distribution was constructed for each individual E-id, and fit with a Gaussian to determine the energy difference for each E-id. The resulting values of  $[E_{\text{True}} - E_{\text{Measured}}]$  versus  $E_{\text{Measured}}$  are shown in Fig. 9

The energy difference is typically less than  $\pm 100$  KeV and always less than  $\pm 0.5$  MeV. This energy difference is a measure of how well the energy center of an E-id is determined. The actual resolution of any E-id will be determined by the physical size of an E-id and will be on the order of an MeV.

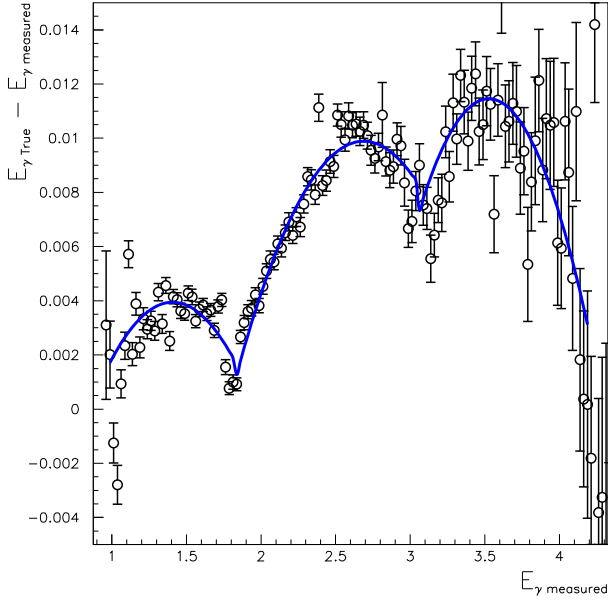


FIG. 6: Left panel:  $[E_{True} - E_{Measured}]$  vs.  $E_{Measured}$  determined by the algorithm detailed here for g8b data. Right panel:  $[E_{True} - E_{Measured}]$  vs. E-id after energy correction has been applied. (All units are GeV.)

TABLE I: Pull parameters from the FSU kinematic fitter.

Particle	Variable	Before energy correction		After energy correction	
		Mean	$\sigma$	Mean	$\sigma$
Proton	p	0.1696	0.9969	0.024	1.018
	$\lambda$	-0.03745	0.9642	-0.043	1.02
	$\varphi$	-0.1447	0.9742	0.0048	1.016
$\pi^+$	p	-0.1655	0.9695	-0.062	1.000
	$\lambda$	-0.04911	0.9663	-0.049	1.022
	$\varphi$	-0.3304	0.9833	-0.083	1.003
$\pi^-$	p	-0.1929	0.9656	-0.0513	1.004
	$\lambda$	-0.01394	0.9715	-0.02	1.026
	$\varphi$	-0.3271	0.9798	-0.058	1.004
$\gamma$	$E_\gamma$	0.3027	1.219	0.0049	1.040

## VII. CONCLUSION

The energy corrections for the g8b data set have been determined by use of a simple iterative routine and verified using the FSU kinematic fitter. The energy center of any given E-id is found to be (after correction) better than  $\approx 0.5$  MeV.

## VIII. ACKNOWLEDGMENTS

This work was supported at Arizona State University by the National Science Foundation award PHY-0653630, and at Florida State University by the Department of Energy award DE-FG02-92ER40735.

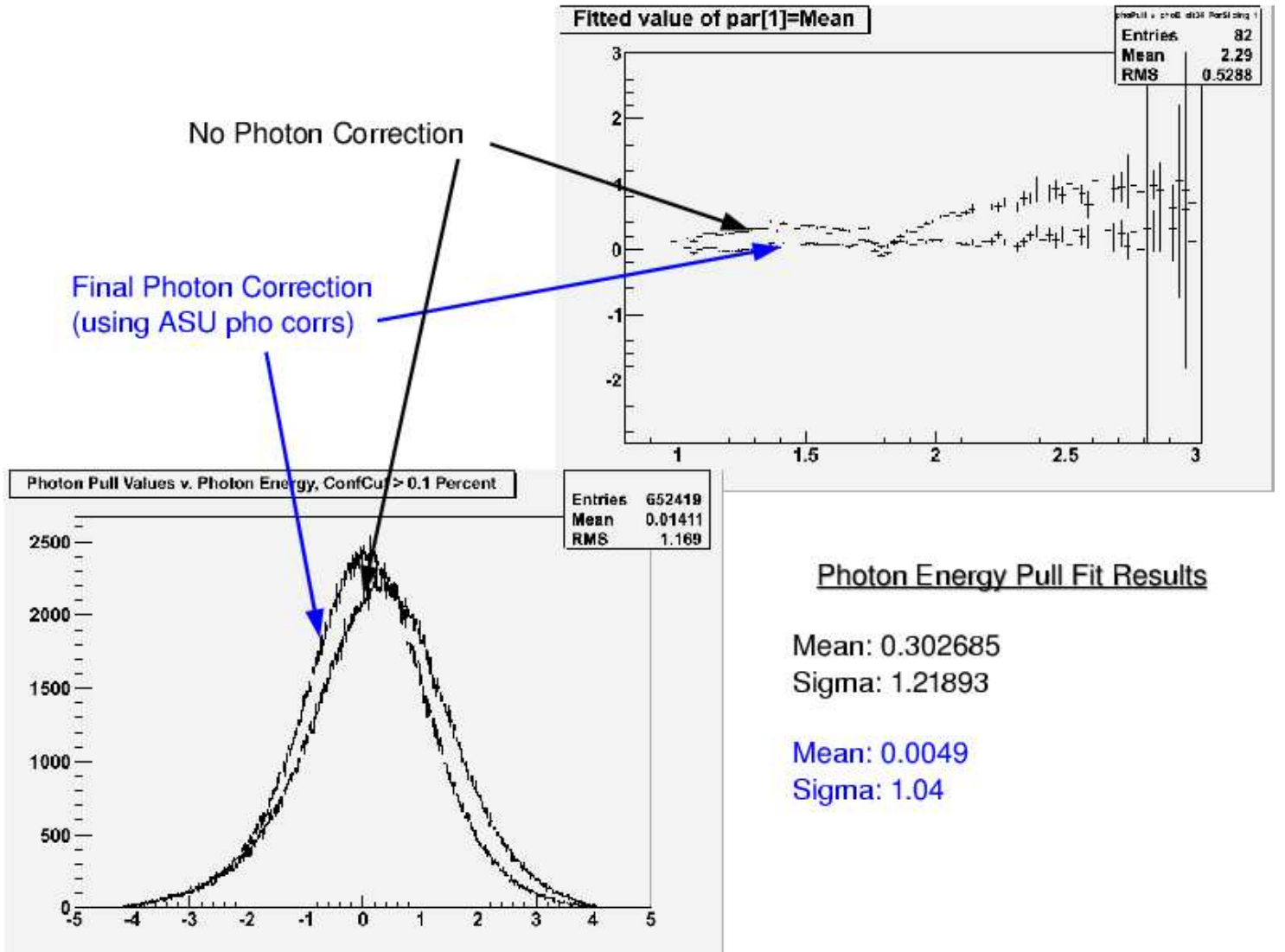


FIG. 7: Lower left panel: Pull distribution for  $E_\gamma$  before and after energy correction has been applied. Upper right panel: Pull values for  $E_\gamma$  before and after energy correction has been applied as a function of  $E_\gamma$  (GeV).

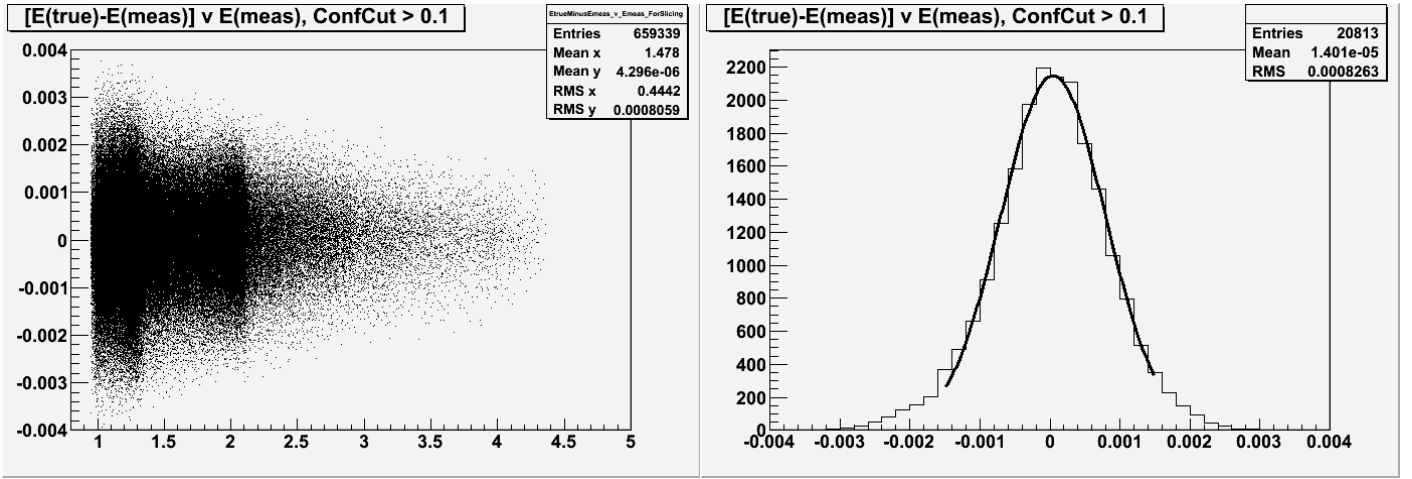


FIG. 8: Left panel: Distribution of  $[E_{\text{True}} - E_{\text{Measured}}]$  versus  $E_{\text{Measured}}$  determined by the FSU kinematic fitter. Right panel: Distribution of  $[E_{\text{True}} - E_{\text{Measured}}]$  for  $E_{\text{Measured}} = 1.3$  GeV. Note:  $E_{\text{True}}$  is determined by the kinematic fitter after the energy corrections have been applied and all energies are in terms of GeV.

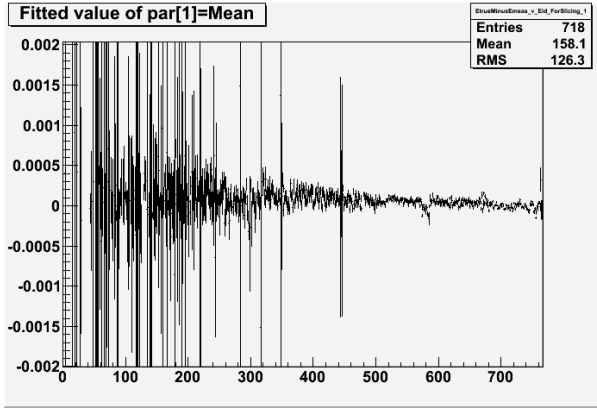


FIG. 9: Left panel:  $[E_{\text{True}} - E_{\text{Measured}}]$  vs.  $E_{\text{id}}$ . Note: vertical scale is in GeV.

---

[1] M. Williams, D. Applegate, C.A. Meyer, CLAS Note 2004-017, [www1.jlab.org/ul/Physics/Hall-B/clas/public/2004-017.pdf](http://www1.jlab.org/ul/Physics/Hall-B/clas/public/2004-017.pdf).